RESEARCH ARTICLE

Device for Assessing Knee Joint Dynamics During Magnetic Resonance Imaging

Sandeep P. Jogi, MT,[1,2] Rafeek Thaha, ME,[1] Sriram Rajan, MD,[3] Vidur Mahajan, MBBS, MBA,[3] Vasantha K. Venugopal, MD,[3] Amit Mehndiratta, PhD,[1,4] and Anup Singh, PhD[1,4]*

Background: Knee assessment with and without load using magnetic resonance imaging (MRI) can provide information on knee joint dynamics and improve the diagnosis of knee joint diseases. Performing such studies on a routine MRI-scanner require a load-exerting device during scanning. There is a need for more studies on developing loading devices and evaluating their clinical potential.
Purpose: Design and develop a portable and easy-to-use axial loading device to evaluate the knee joint dynamics during the MRI study.
Study Type: Prospective study.
Subjects: Nine healthy subjects.
Field Strength/Sequence: A 0.25 T standing-open MRI and 3.0 T MRI. PD-T_2-weighted FSE, 3D-fast-spoiled-gradient-echo, FS-PD, and CartiGram sequences.
Assessment: Design and development of loading device, calibration of loads, MR safety assessment (using projectile angular displacement, torque, and temperature tests). Scoring system for ease of doing. Qualitative (by radiologist) and quantitative (using structural similarity index measure [SSIM]) image-artifact assessment. Evaluation of repeatability, comparison with various standing stances load, and loading effect on knee MR parameters (tibiofemoral bone gap [TFBG], femoral cartilage thickness [FCT], tibial cartilage thickness [TCT], femoral cartilage T_2-value [FCT2], and tibia cartilage T_2-value [TCT2]). The relative percentage change (RPC) in parameters due to the device load was computed.
Statistical Test: Pearson's correlation coefficient (*r*).
Results: The developed device is conditional-MR safe (details in the manuscript and supplementary materials), $15 \times 15 \times 45$ cm^3 dimension, and <3 kg. The ease of using the device was 4.9/5. The device introduced no visible image artifacts, and SSIM of 0.9889 ± 0.0153 was observed. The TFBG intraobserver variability (absolute difference) was <0.1 mm. Interobserver variability of all regions of interest was <0.1 mm. The load exerted by the device was close to the load during standing on both legs in 0.25 T scanner with r > 0.9. Loading resulted in RPC of 1.5%–11.0%, 7.9%–8.5%, and −1.5% to 13.0% in the TFBG, FCT, and TCT, respectively. FCT2 and TCT2 were reduced in range of 1.5–2.7 msec and 0.5–2.3 msec due to load.
Data Conclusion: The proposed device is conditionally MR safe, low cost (material cost < INR 6000), portable, and effective in loading the knee joint with up to 50% of body weight.
Evidence Level: 1
Technical Efficacy: Stage 1

J. MAGN. RESON. IMAGING 2022;55:895–907.

The knee joint is an essential load-bearing joint that facilitates the mobility of an individual. Magnetic resonance imaging (MRI) provides imaging-derived measures of morphological and biochemical characteristics of various tissues in the knee joint and has wide use in clinical studies and research.[1–4] Routine clinical MRI studies are conducted in the supine position, without any load on the knee joint.[5] However, a comparative analysis of the knee joint images acquired during load and without load can provide additional information about joint characteristics.[6–8] Standing-open MR

View this article online at wileyonlinelibrary.com. DOI: 10.1002/jmri.27877

Received Feb 25, 2021, Accepted for publication Jul 27, 2021.

*Address reprint requests to: A.S., Centre of Biomedical Engineering, Indian Institute of Technology Delhi, Hauz Khas, New Delhi-110016, India. E-mail: anupsm@iitd.ac.in

From the [1]Centre for Biomedical Engineering, Indian Institute of Technology Delhi, New Delhi, India; [2]Department of Biomedical Engineering, ASET, Amity University Haryana, Gurgaon, Haryana, India; [3]Mahajan Imaging Centre, New Delhi, India; and [4]Department of Biomedical Engineering, All India Institute of Medical Sciences, New Delhi, India

Additional supporting information may be found in the online version of this article

scanners can scan the knee joint with a load, but images have a lower signal-to-noise ratio (SNR), and systems have limited availability.[9–13] Some recent studies have used MR compatible knee joint loading device[8,14–17] to assess the knee loading effect. Further research studies are required to improve a loading device to simulate load during MRI scanning and its potential for clinical studies.

Multiple studies have shown changes in the knee joint load-bearing tissues during loading.[14–16,18–24] Load-induced changes were reported in the tibiofemoral bone gap, cartilage thickness, meniscal extrusion, and quantitative MRI parameters such as T1rho and T_2 values.[14–16,18–27] Additionally, differences in the knee joint MRI parameters due to load have been reported[14,22–24,27] among healthy subjects and osteoarthritis patients. Such studies require a mechanism to load the knee joint during an MRI scan.

The pain in the knee joint arises in stress conditions; therefore, imaging during the load on the knee joint is significant for diagnosis.[28] Further, previous studies[29–31] reported diagnostic mismatches between unloaded and loaded knee imaging. From a clinical perspective, loading experiments might improve the diagnosis of osteoarthritis (OA) in the early stage. Femoral cartilage thickness and tibiofemoral bone gap were found to decrease in loading condition, more in subjects with mild-to-moderate OA condition than the subject without OA.[22] Similarly, an increase in the meniscus extrusion was reported in KL score = 0, 1, and 3.[23] Loading of knee joint reduced the T1rho and T_2 values of the superficial layer of cartilage largely in subjects with mild OA (KL score = 1) compared to healthy subjects.[24] Further studies to evaluate the clinical significance of the changes due to loading are required. However, such studies are limited mainly due to loading devices such as lack of commercial availability, expensive devices, and difficulty to set up. Therefore, more studies are required to develop novel loading devices, which are easy to use in regular clinical settings.

Studies have reported the design of the knee joint loading devices and the loading effect of 50% of body weight (50% BW)[8,14–17] on the knee joint. The loading device reported by Nag et al,[8] Souza et al,[14] and Nishii et al[15] had a bulky design mechanism. Whereas the device design described by Wang et al[16] consists of an MRI-compatible load cell to measure load and a motorized rod to transfer the load to the body. Furthermore, the knee loading apparatus by Lange et al[17] has an arrangement whereby the subject applies force against a fixture to exert load. However, each of these devices[8,14–17] has a few limitations. These reported knee joint loading devices[8,14–17] are bulky and require significant time to set up in the MRI room or required alterations in the MRI room setting[16]; therefore, it is difficult to use them in a standard clinical setting.

Moreover, the reported devices[8,14–17] apply a load from one direction that may push the subject in one direction, which may develop motion artifacts during scanning.[17] Lange et al[17] use an additional optical arrangement to track such motion. Thus, there is a requirement for a new device that can address some of the limitations of earlier reported devices.[8,14–17]

Thus, the aims of this study were to design and develop an MR-safe axial knee joint loading device that should be portable, easy to put on and take off, and low cost.

Materials and Methods

Nine healthy male subjects with no history of knee injury or any knee pathology such as OA, were enrolled for the experiment with prior approval from Institutional Review Board (IRB) and informed written consent of the subjects.

Design and Development of Loading Device

The proposed device consists of: 1) a waist belt made of synthetic fiber (Nylon), 2) wooden foot rest and calf rest, 3) a nonferromagnetic stainless-steel (SS-304) telescopic-channel, 4) a nonelastic string of synthetic fiber (Nylon), and 5) an elastic string of synthetic rubber (Domyos Pvt. Ltd., Lille, France). A computer aided design (CAD) model of the proposed device was developed. The foot rest is placed at the plantar aspect of the subject's foot, which exerts a load on the foot sole. The waist belt and the foot rest are connected with an adjustable nonelastic and an elastic string. Additionally, the calf rest was designed to accommodate the calf muscle, connected to the foot rest by telescopic-channel, that provides the direction for exerted load from the foot sole to the tibial bone axis. The cost of each component used for design was listed in the section 5 of the Supplementary Material.

MR Safety Assessment

The proposed device is a passive, nonimplantable, nonferromagnetic, and nonelectrical type. The telescopic channels are tightly tied with the calf rest and the foot rest; thus, there are no loose components. Further, MR safety assessment has been done for projectile motion and developed torque in statics magnetic field and heat generation due to radiofrequency (RF) and gradient coil exposure during scanning as per American Society for Testing and Materials (ASTM) standard guidelines, as shown in Figure 1 (details of MR safety testing experiments given in the section 1 of the Supplementary Material).

The string suspension method[32] was used for projectile motion assessment at clinical MRI scanners of 1.5 T and 3.0 T, as shown in Figure 1(a). The angular displacement of the string was measured by the protractor as shown in Figure 1(a). In addition, the torque of the device was observed using both the string suspension method and the device at a frictional surface.[33] Further, the device was also tested in experimental conditions in which the device was tied with the MRI table using straps.

A noncontact infrared thermometer (Nureca Ltd., Mumbai, India) (input range: 0–100°C, resolution: 0.1°C) was used to measure the heat generation, due to the loading device, during MRI scanning at 3 T. Temperature measurements were taken before and after MRI scanning (3.0 T MRI) on the surface of a phantom that is GE 5342680 (GE Medical System, MR division, 3200 N Grandview Bivd, Waukesha, WI, USA). The phantom was inside MRI scanner room for more than 24 hours and the loading device was kept in the MR scanner room for 1 hour before temperature

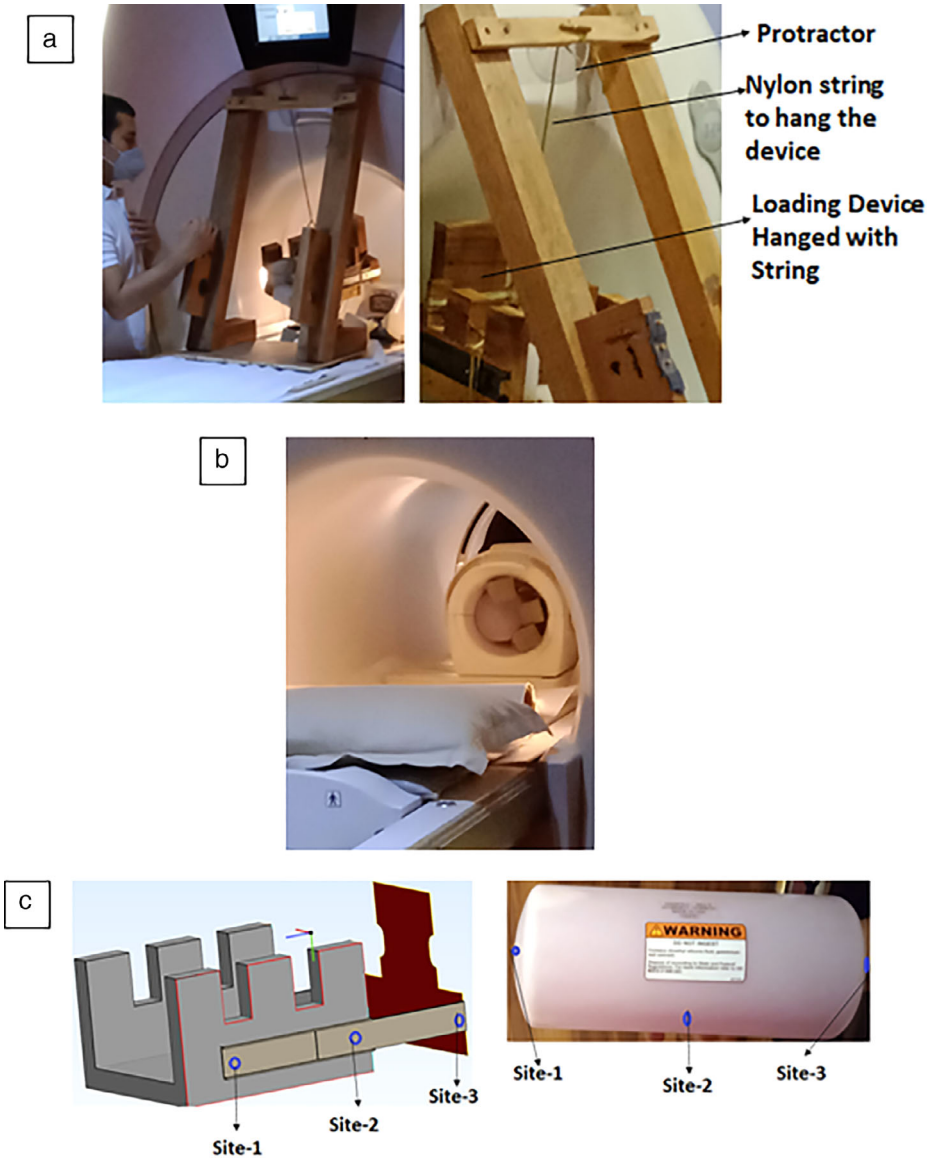

FIGURE 1: The experimental setups for MR safety assessment. (a) The experimental setup arrangement for projectile motion and torque assessment; a plastic protractor was used to measure angular displacement, and the loading device was suspended with a thin nylon string. (b) Scanning of the device with phantom for temperature change assessment using 3.0 T MRI. (c) Three respective sites of temperature observe at the loading device metallic component (left) and a phantom (right).

measurements. The phantom was placed inside the same RF coil, and phantom scanning was performed using the same protocol as used for human subjects. This experiment was to evaluate the heating of the loading device due to RF and gradient coil,[34] as shown in Figure 1(b). A reference device was also placed inside the MRI near corner (outside 5 Gauss field) to observe any change in temperature due to the temperature controller of the MRI room. The surface temperature was measured at three sites: two extreme ends, one at the middle of each phantom, and the device as shown in Figure 1(c). The temperature change was evaluated as the difference between before and after MRI scanning. Measurements were repeated three times, and values were reported as average of these.

During the experiment, the subjects were also asked whether they feel any heat or pull during scanning.

Calibration of the Loading Device

A calibration table for the applied load versus length of stretched elastic string ("x") was generated using a digital traction machine (DIGITRAC, HMS Medical Systems, Chennai, India) (Supplementary material Section 2 provides the specification of traction machine and Supplementary Figure 1 shows the image of traction machine) and a ruler with millimetric resolution. The digital traction machine was used to apply constant load on the elastic string, and then the length of the stretched elastic string was manually measured against each applied load. The load was applied over the range of 3–45 kg in incremental steps of 1 kg. Each step load was applied for 15 minutes (Supplementary Figure 2 shows the schematic of calibration experiment setup). Moreover, before applying the next step load, a complete release-off load was performed. The calibration

process was repeated five times with a gap of more than 24 hours. An average of five repetitions was used to prepare a calibration look-up table for applied load *versus* stretched length. The obtained data were also fitted with different mathematical functions such as exponential function, power function, and polynomial functions of first, second, third, fourth, and fifth order to find the best calibration curve using Akaike information criterion (AIC) and AIC corrected (AICc).[35]

50% BW was loaded on the knee joint of healthy human subjects. Firstly, the individual subject's weight was measured, then

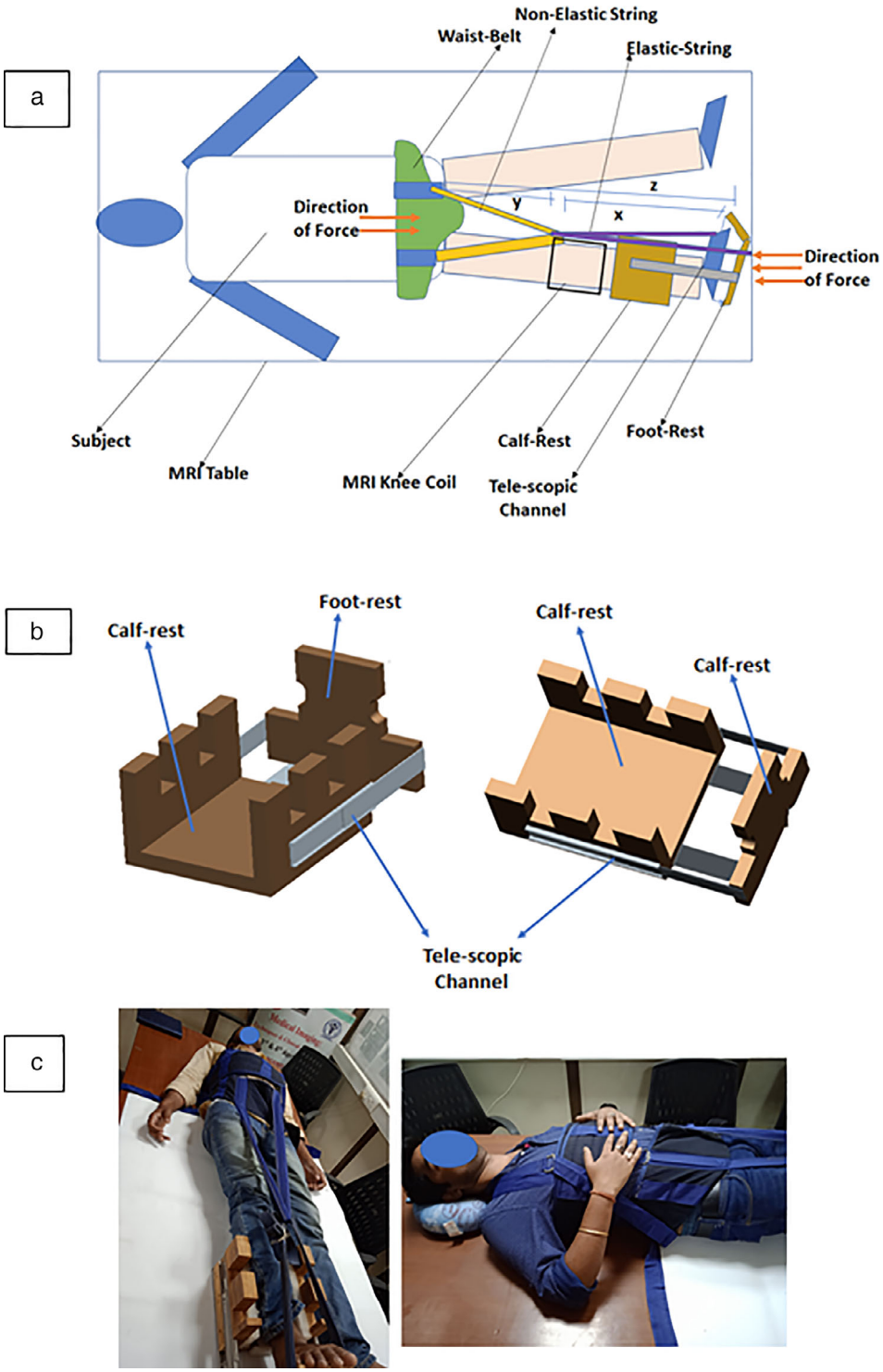

FIGURE 2: (a) The proposed loading device and its attachment to the subject. (b) An isometric view of the proposed device on the left side and a top view on the right side. An adjustable telescopic-channel connects the foot rest and the calf rest. (c) The device's loading mechanism during laboratory testing (on the left-hand side) and securely wrapped waist belt during testing (on the right-hand side).

determined the stretched length of elastic string ("x") for 50% BW using the calibration chart. Second, the length between the waist belt and foot rest was measured as "*z*." Finally, fix the adjustable non-elastic string at "y," such that $y = z - x$, where "*x*" is responsible for the applied force, as shown in Figure 2(a).

The device was assessed for the ease of donning (put on and take off on the subject to be scanned) and degree of comfort (the comfort of the subject to applied load using the device). For ease of doing experiment, an average score of three metrics: the time for device put on (within 5, 7.5, 10, 12.5, 15 minutes), device take off time (within 1, 2, 3, 4, 5 minutes), and perception of individual ease (very easy, easy, neutral, difficult, and very difficult), each on the scale of 5 was evaluated respectively (Supplementary material section 3 described details of ease of doing experiment). Similarly, the degree of comfort was evaluated on the scale of 5 (5 to 1 as: absolutely comfortable with applied load, can manage the applied load with minimum unease, can manage the applied load with moderate unease, can manage the applied load with pain, cannot manage the applied load with high pain, respectively) for five-time intervals (0–5, 5–15, 15–25, 25–35, and 35–45 minutes) (Supplementary material section 4 described details of this experiment).

In the current study, the durability of the elastic string was tested for 1 year and on multiple subjects.

MRI of Subjects at 3 T and 0.25 T

The study was conducted using a 3.0 T MRI scanner (General Electric Healthcare, Chicago, Illinois) with an 8-channel knee coil

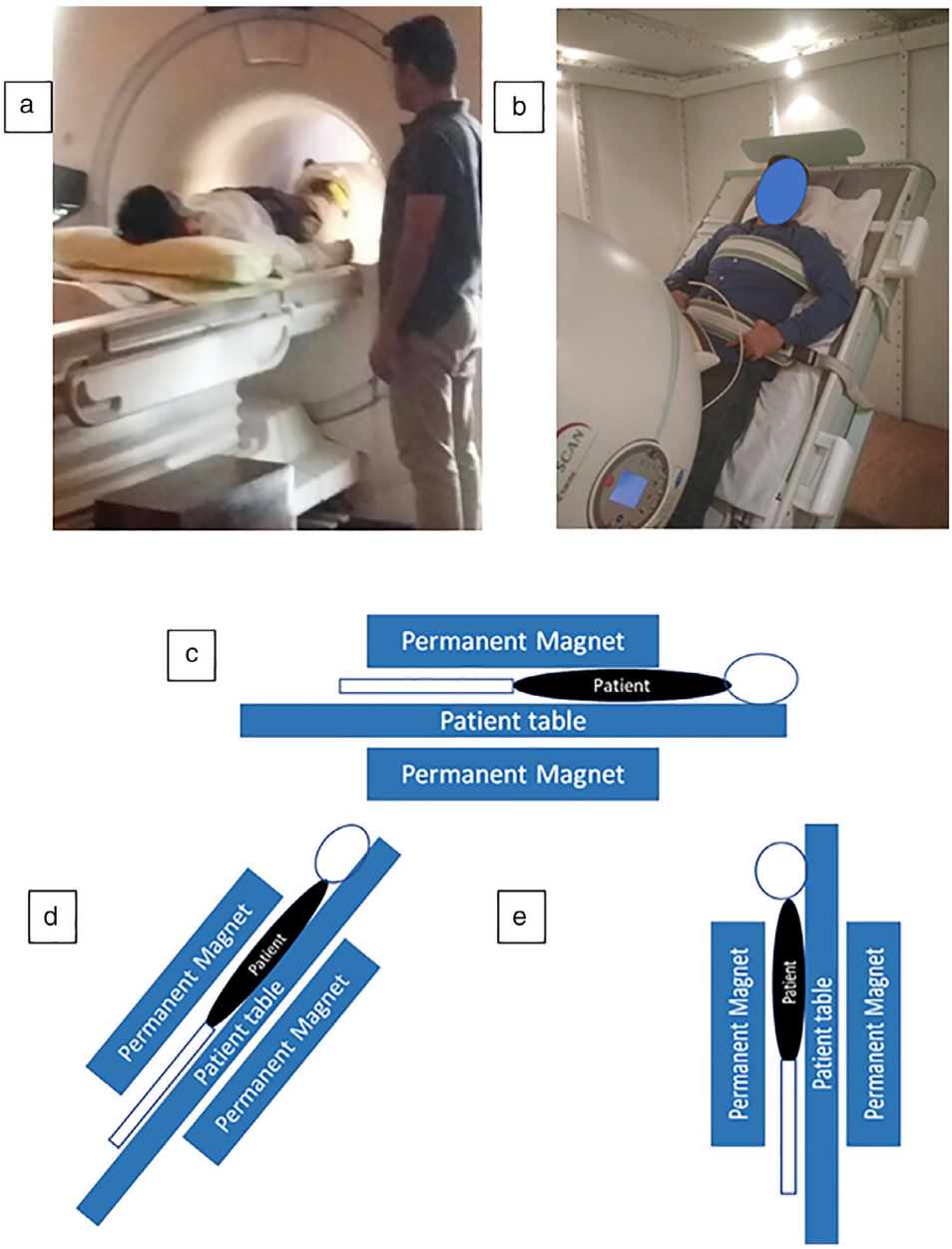

FIGURE 3: (a) The scanning in 3.0 T MRI. (b) The scanning in 0.25 T open-standing MRI. (c–e) The schematic of a subject position inside open MRI as a supine position, 45° aligned, and 84° aligned, respectively.

(Figure 3(a)) and on a 0.25 T (Figure 3(b)), an open standing MRI scanner (G-Scan, Estaote, Genova, Italy).

MRI data of three out of nine subjects were acquired at 0.25 T in coronal orientation using dual proton density-T_2-weighted (PD-T_2) fast spin echo (FSE) sequence (repetition time [TR] = 4260 msec, echo time [TE] = 25 msec/100 msec, the field of view [FOV] = 210 × 210 mm^2, reconstructed image matrix = 512 × 512, slice thickness = 3.5 mm, number of slices = 19). At 0.25 T scanner, subjects were scanned in a supine position with 50% BW load exerted using the device (Figure 3(c)). For comparison purposes, the same subjects were scanned at 45° aligned and 84° aligned positions (without loading device), as shown in Figure 3(d,e). The position chosen for the scan exerts a different load on the subject's knee, as explained in the experiment protocol in Table 1. The subject knee joint was loaded around 10 minutes for each position before acquiring images in the loading condition. Two repetitions of MRI data at 0.25 T, for two subjects, were acquired with a gap of 1 hour.

MRI data of all nine subjects were acquired at 3.0 T in coronal orientation using fat saturated 3D-fast spoiled gradient echo (FSPGR) sequence (TR = 10.8 msec, TE = 3.5 msec, FOV = 140 × 140 mm^2, reconstructed image size = 512 × 512, slice thickness = 2 mm, number of slices = 72), multiecho T_2-weighted FSE (TR = 1500 msec, TE = 6.4, 12.8, 19.2, 25.6, 32, 38.4, 44.8, and 51.2 msec, FOV = 140 × 140 mm^2, reconstructed image matrix = 256 × 256, slice thickness = 3 mm, number of slices = 20), and fat suppressed proton density (FS-PD) images (TR = 2881 msec, TE = 8.9 msec, FOV = 140 × 140 mm^2, reconstructed image matrix = 512 × 512, slice thickness = 3 mm, number of slices = 30). Each subject was scanned in a supine position without and with 50% BW load using the device. Summary of the experiment protocol is presented in Table 1.

The Device-Induced Artifact Assessment

The device-induced MR image changes were assessed by comparing the MR image acquired with and without the loading device. Three experts with 19 years (S.R.), 11 years (V.K.V.), and 4 years of experience evaluated the loading device-induced artifact and image quality changes in images of spin-echo sequence and gradient-echo sequences. Qualitative assessment of artifact by radiologists graded as 1) no visible artifact: score 3, 2) artifact visible but does not affect clinical decision-making: score 2, and 3) artifact visible and affect clinical decision-making: score 1. For image quality, radiologists assessed noise, contrast, and spatial resolution as 1) no difference visible: score 4, 2) small difference, does not affect clinical findings: score 3, 3) small difference, possibly affect clinical findings: score 2, and 4) substantial difference, affecting clinical findings: score 1. The mean and standard deviation of three radiologist score were reported for artifacts and image quality. Further, for quantitative evaluation, three registered images of unloaded and loaded were used from the anterior, middle, and posterior slices of each data set for the structural similarity index measure (SSIM)[36] using the following equation:

$$\mathrm{SSIM}(x,y) = \frac{(2\mu x\mu y + C1)(2\sigma xy + C2)}{(\mu 2x + \mu 2y + C1)(\sigma 2x + \sigma 2y + C2)} \quad (1)$$

where μ_x and μ_y are the local means; σ_x and σ_y are the standard deviations; σ_{xy} is the cross-covariance for images x and y; C_1 and C_2 coefficients are a function of the dynamic range of intensity of images (I).

$$C1 = (0.01 \times I)^2 \quad (2)$$

TABLE 1. Experimental Protocol of the Study

0.25 T Standing Open-MRI	3.0 T MRI
• Laydown supine position, without weight (repeat with gap of 1 hour) • SB45: Standing on both leg against gravity at 45° aligned (35% of body weight) • SB84: Standing on both leg against gravity at 84° aligned (49% of body weight) • SS84: Standing on single leg against gravity at 84° aligned (99% of body weight) • Using device: Loading in laydown supine position using proposed loading device (50% of body weight; repeat with gap of 1 hour)	• Laydown supine position without weight • Using device: Loading in laydown position using proposed loading device (50% of body weight)
Parameter Evaluate	Parameter Extract
• Tibiofemoral-bone-gap (TFBG): Using PD-T_2 dual sequence images • The repeat scan of the supine position scanning, without load and with load using the device, use for evaluating reproducibility and robustness of the knee joint measurement method of TFBG	• Tibiofemoral-bone-gap: Using FSPGR images • Femoral-cartilage-thickness: Using FS-PD images • Femoral-cartilage T_2-Value: Using CartiGram images

$$C2 = (0.03 \times I)^2 \quad (3)$$

Finally, SSIM can be represented as a map for the visual assessment of artifacts. The means and standard deviation of SSIM value were computed for all the dataset.

Data Analysis

MR images were processed for computing tibiofemoral bone gap (TFBG), femoral cartilage thickness (FCT), tibial cartilage thickness (TCT), femoral cartilage T_2 values (FCT2), and tibial cartilage T_2 values (TCT2) at each medial and lateral compartment. The region of interest (ROI) was segmented by two observers (S.P.J. and R.T.), and interobserver variability was evaluated. Segmented ROIs were validated by the radiologist (S.R.). Each parameter was computed at the ROI of the images using a semi-automatic in-house-built routine on MATLAB R2018a (The MathWorks Inc., Natick, MA, USA). The ROI was segmented from the trochlea to the posterior femur condyles till the visibility of the meniscus.

For TFBG evaluation, the tibiofemoral bone gap ROI's normal gap between each pixel of interface with bones was measured for each slice and then fed in a 2D-WearMap row.[37] Further, the average of TFBG at four regions on bone gap 2D-WearMap: 1) the whole lateral and medial compartment profile and 2) lateral and medial regions where femur cartilage makes contact with tibial cartilage were computed. Figure 4 shows the pipeline of data analysis.

Similarly, FCT and TCT of each region were computed from the cartilage-thickness 2D-WearMap. The cartilage-thickness 2D-WearMap was developed by feeding the values of tangential thickness at each pixel where cartilage interfaces with bone for each slice, as shown in the steps of Figure 4. The procedure of generating 2D-WearMap is described in the reported study.[37]

Similarly, FCT2 and TCT2 of each region were evaluated from the 2D-WearMap of the cartilage's T_2-value map. The T_2-map or CartiGram was generated by fitting mono-exponential function[37] given as follows:

$$S(\mathrm{TE}) = S_0 \times e^{-(\mathrm{TE}/\mathrm{T}_2)} + c \quad (4)$$

where $S(\mathrm{TE})$ is the signal intensity of the T_2-weighted image at echo time (TE); T_2 is the transverse relaxation time, S_0 is the initial signal intensity, and c is a constant are parameters to be estimated. The 2D-WearMap of the cartilage's T_2-value map was developed by averaging the T_2-values across tangential cartilage thickness, as shown in the steps of Figure 4.

Finally, the loading effect on the knee joint was evaluated as the relative percentage change (RPC) of these parameters using the following equation:

$$\mathrm{RPC} = \frac{V1 - V2}{V1} \times 100 \quad (5)$$

$V1$ and $V2$ in the Eq. 5 represent the average value of unloaded and load parameters (FTBG, FCT, TCT, FCT2, and TCT2) in the corresponding region.

For 0.25 T MR images, only the FTBG parameter was computed. A repeat scan of two out of three subjects, without and with

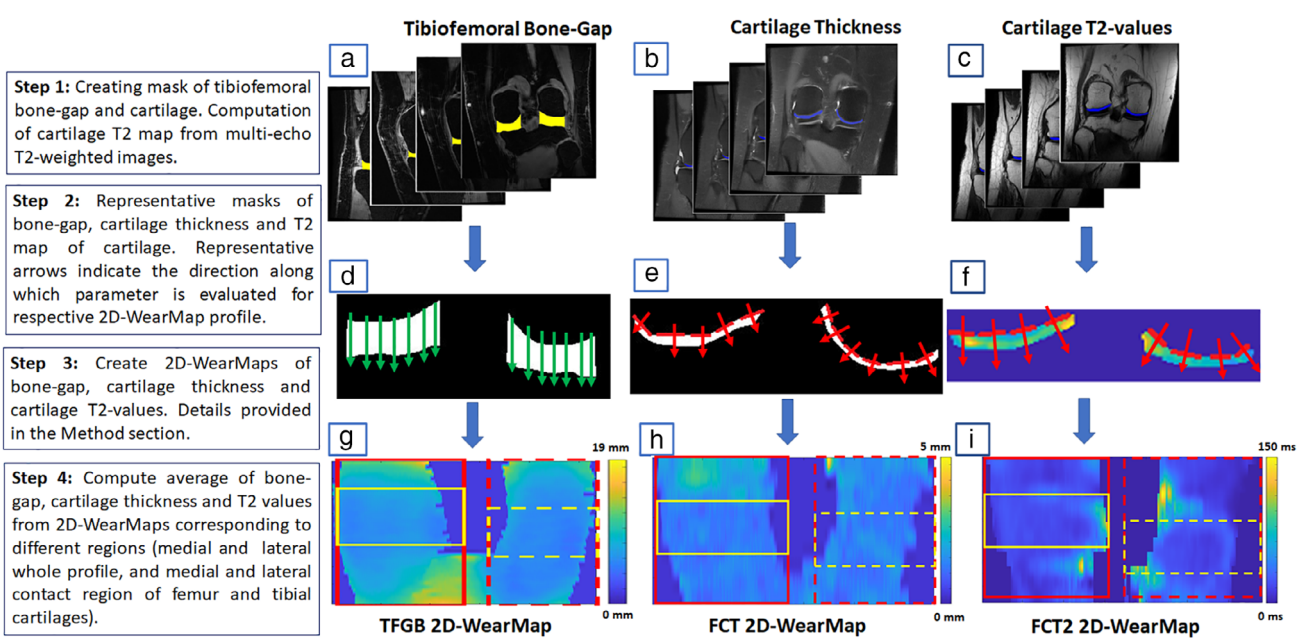

FIGURE 4: Flow chart of data processing for generating TFBG, FCT, TCT, FCT2, and TCT2; (a) shows overlay of bone gap on SPGR image, (b) and (c) show overlay of cartilage thickness on FS-PD and T_2-weighted images, respectively; (d) and (e) show representative masks of bone gap, cartilage thickness, and (f) shows map of cartilage T_2-values; the green arrows in (d) show the bone gap is evaluated normal to each pixel, red arrows in (e) represent the cartilage thickness is evaluated normal to tangent at each pixel of bone cartilage interface, and red arrows in (f) show the cartilage T_2-value evaluated as average across normal to tangent of each pixel bone cartilage interface; (g–i) shows 2D-WearMaps for bone gap, cartilage thickness, and cartilage T_2-values, respectively. Rectangular boxes on (g–i) represent the whole lateral region (red box), the whole medial region (red-dotted line) of each 2D-WearMap; lateral and medial regions of each 2D-Wearmap where both cartilage contact with each other shows in yellow box and yellow-dotted line, respectively.

a load in the supine position, has also been performed using 0.25 T MRI. To test the repeatability, the mean difference between the two scans was calculated for medial and lateral FTBG.

Statistical Analysis

The mean and standard deviation of values from the entire SSIM map was computed. The interobserver and intraobserver variability of segmented ROI was evaluated in four metrics: mean difference and standard deviation; absolute difference and standard deviation; relative percentage difference and standard deviation; and relative absolute difference and standard deviation.[38] Using 0.25 T MR images, the FTBG obtained with the loading device was compared with the respective FTBG obtained with natural load at various stances, using Pearson's linear correlation coefficient "*r*," to understand the comparative knee's mimicked position under the device's load.

Results

A low-cost (material cost < INR 6000 or <$100)(Supplementary material Section 5), portable, lightweight axial knee joint loading device was designed and developed successfully with a dimension of 15 × 15 × 45 cm^3 with the weight of lesser than 3 kg, as shown in Figure 2. The nine healthy subjects (age: 24–38 years, weight: 65–80 kg, and height: 1.65–1.75 m) were scanned with the loading device.

The waist belt is designed to securely wrap around the subject's waist, as shown in Figure 2(a). A CAD model of the loading device is shown in Figure 2(b). Stretched elastic string develops traction force between the subject's waist and the foot sole, as shown in Figure 2(a,c). Consequently, a force produces at the knee joint, equivalent to the tensional force of stretched elastic string. The developed device is very easy to use with a score of ease of doing 4.9 on the scale of 5, required 2.0–2.5 minutes put on time, and less than 1 minute to take off (detailed results are shown in Supplementary Table 5). The applied load of the device is comfortable for the subject up to 15 minutes with minimum unease and up to 25 minutes with moderate unease (detailed results are shown in Supplementary Table 6).

Calibration of Elastic String

The average of five repeat calibration outcomes is shown in Figure 5 (Supplementary material Section 6 shows results of five repeat calibration outcomes.). The coefficient of variation during calibration was evaluated as 1.7 ± 0.8 (in %). A second-order polynomial of Eq. 6 was evaluated as the best-fit model using AIC for the calibration data: applied load vs. the length of stretched elastic string.

$$Y = a \times W^2 + b \times W + C \tag{6}$$

where "*Y*" is the stretched length of elastic string; "*W*" is the desired load to be applied; "a," "b," and *C* are coefficients with value 0.027, 0.126, and 23, respectively. In each iteration of calibration, the obtained stretched length of the elastic string against each applied step load was confined within a 95% confidence graph of the polynomial fit, as shown in Figure 5.

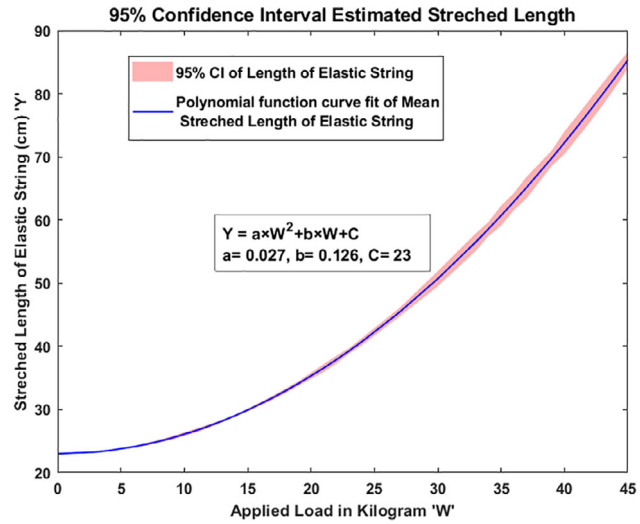

FIGURE 5: Shows graph (with 95% confidence interval) of the stretched length of elastic belt vs. applied load and fitted polynomial function.

In the current study, no changes in the calibration parameters were observed over 1 year.

MR Safety Assessment

The average angular displacement of three readings during the projectile motion test was measured as 14° ± 0.47 and 36° ± 0.47 in 1.5 T and 3.0 T MRI, respectively (result is given in Supplementary material Section 1 and Supplementary Table 1). Torque has been observed both during string suspension method and free device placement on MRI-table in 1.5 T and 3.0 T MRI. However, no torque was observed in the experimental condition when the device is tied with the MRI table (detail of result is given in Supplementary material Section 1 and Supplementary Table 2). In the assessment of heat generation, an increase in the temperature of the device and phantom was observed as 0.1°C. (detail result is given in Supplementary material Section 1 and Supplementary Table 3). None of the scanned subjects reported any heating or pulling force of the device (magnetic attraction) during the MRI scanner at 0.25 T and 3.0 T.

Assessment of Artifacts Due to Loading Device

The radiologists reported no visible artifacts (3.00 ± 0.00 out of 3) due to the loading device in images of spin-echo, and artifact visible but does not affect clinical finding (2.33 ± 0.47 out of 3) in images of gradient-echo sequences. Radiologists evaluated the comparison of quality of images acquired without and with the loading device as "small changes, doesn't affecting clinical finding" in both spin-echo

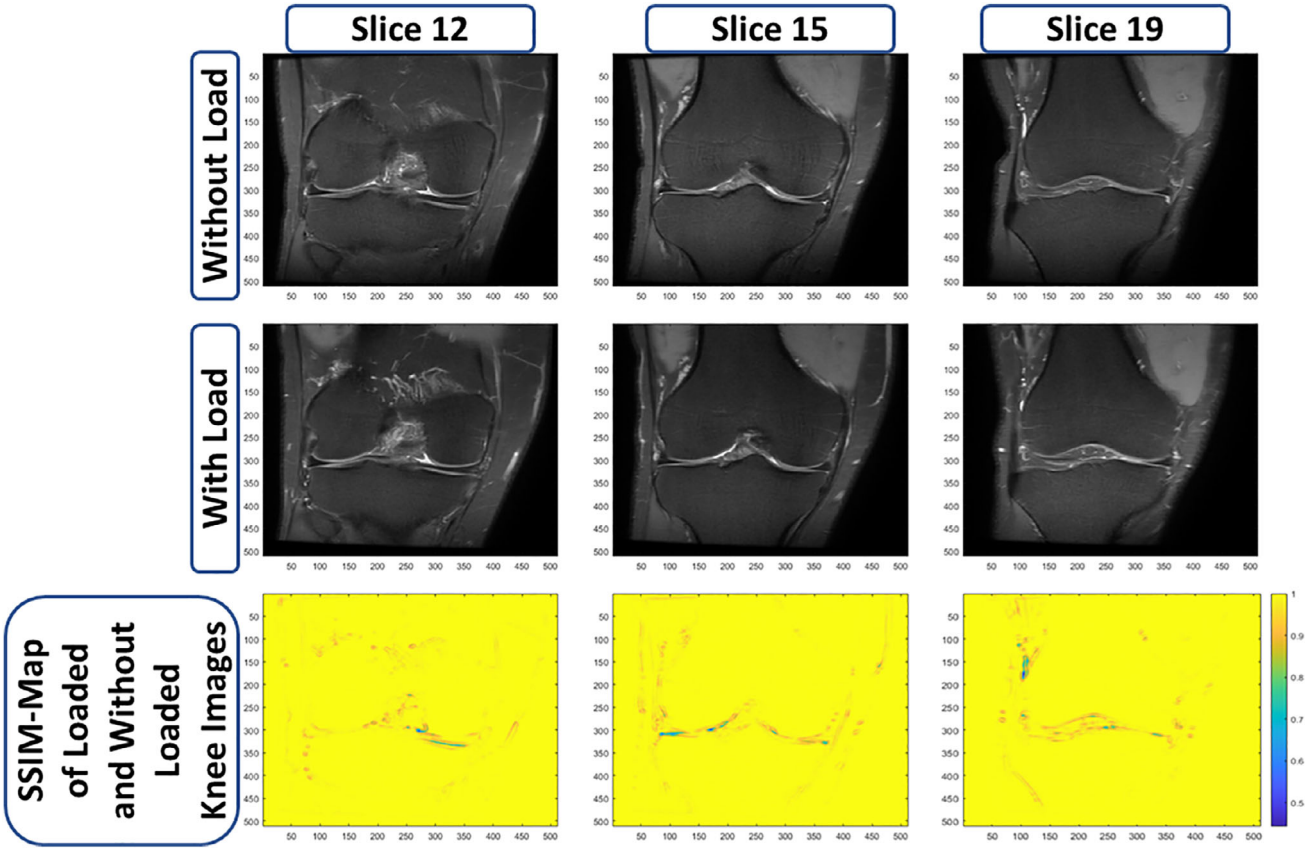

FIGURE 6: Similarity index mapping (SSIM) between MR images acquired using the loading device and without loading device for representative slices of the knee joint of a healthy subject.

sequence (3.55 ± 0.49 out of 4) and gradient-echo sequence images (3.22 ± 0.62 out of 4). In quantitative evaluation, SSIM of 0.9889 ± 0.0153 shows the proposed loading device introduced no artifacts, and image quality was similar to without the loading device. Figure 6 shows the similarity index maps for different slices.

Unloading vs. Loading Using 0.25 T MRI

The intraobserver variability of FTBG evaluation is shown in Table 2. Repeatability of FTBG measurement without load provided a mean difference of 0.03 mm and 0.01 mm in medial and lateral FTBG, respectively. Similarly, repeatability of FTBG measurement with loading using device observed

TABLE 2. Observer Variability of Each Segmented Region of Interest

		All Measurements are in Millimeter (mm)			
		Difference	Absolute Difference	Relative Difference %	Relative Absolute Difference %
Region of Interest		$(A-B)$	$\lvert A-B\rvert$	$\frac{A-B}{\frac{A+B}{2}}$	$\frac{\lvert A-B\rvert}{\frac{A+B}{2}}$
Tibiofemoral bone gap (0.25 T)	Intraobserver variability	0.02 ± 0.09	0.07 ± 0.05	0.32 ± 1.70	1.40 ± 1.01
Tibiofemoral bone gap (3.0 T)	Interobserver variability	0.00 ± 0.09	0.07 ± 0.06	−0.04 ± 1.63	1.27 ± 1.03
Femoral cartilage thickness (3.0 T)		−0.03 ± 0.07	0.05 ± 0.05	−2.05 ± 5.06	3.62 ± 4.09
Tibial cartilage thickness (3.0 T)		0.01 ± 0.07	0.06 ± 0.04	0.82 ± 4.22	3.61 ± 2.33

A and B are parameters evaluated of segmented ROI by SPJ and RT, respectively.

TABLE 3. Percentage Changes in Tibiofemoral Bone Gap Corresponding to Various Condition of Loaded Knee Joint With Respect to Rest Position

	Device		SB45		SB84		SS84	
Loading Condition	**L**	**M**	**L**	**M**	**L**	**M**	**L**	**M**
Subject 1	6.99	31.6	5.2	14.18	1.64	20.28	4.93	38.09
Subject 2	−0.21	2.26	−3.27	0.58	−0.11	3.01	4	23.1
Subject 3	9.53	18.82	7.8	12.6	3.25	23.14	8.44	23.83
Mean ± SD	5.4 ± 4.1	17.5 ± 12	3.2 ± 4.7	9.1 ± 6	1.5 ± 1.3	15.4 ± 8.8	5.7 ± 1.9	28.3 ± 6.9
Average of 'r'			0.9706		0.9029		0.8396	

SB45: Standing on both leg against gravity at 45° aligned, SB84: Standing on both leg against gravity at 84° aligned, and SS84: Standing on single leg against gravity at 84° aligned; L and M represent the lateral and medial compartment of the knee joint, respectively; Average of 'r': average of Pearson's correlation coefficient of lateral and medial tibiofemoral bone gap of each stance with respect to tibiofemoral bone gap during device load.

mean difference of 0.08 mm and 0.04 mm in medial and lateral FTBG, respectively.

Table 3 shows the percentage of changes of FTBG between without a load in the supine position and other loading conditions (loading with the device and with natural standing stances). In addition, the table depicts a comparison of the percentage changes of FTBG during various standing stances and alignment (SB45, SB84, and SS84) to device load, with "*r*" as 0.97, 0.90, and 0.83 (with $P < 0.37$), respectively.

Unloading vs. Loading Using 3.0 T MRI

The interobserver variability of each segmented ROI has been given in Table 2. The effect of the loading device as relative percentage changes (RPC) in FTBG, FCT, and TCT of each corresponding region are shown in Table 4. Besides, the mean change of FCT2 and TCT2 in milliseconds at the medial and lateral profile is shown in Table 4.

Discussion

A knee loading study with MRI to access the additional information and dynamic changes in weight-bearing knee requires an MR-safe knee axial loading arrangement. Various clinical applications were suggested in previous reports.[22,24,28–31,39,40] Therefore, the primary objective of the current study was to design and develop a portable and easy in use, axial loading knee joint device, which would be capable of addressing the limitation of previously reported devices[8,14–17]; furthermore, the device has been tested for MR safety, the device induces artifact and change in image quality and the repeatability of the device performance. The secondary objective of the current study was to observe changes in load-bearing tissue of the knee joint using the proposed loading device and conventional 3.0 T MRI.

The proposed device in this study is portable, with a $15 \times 15 \times 45$ cm^3 dimension and less than 3 kg weight, and the device is made up of MRI-safe materials. However, similar devices reported by Nag et al,[8] Nishii et al,[15] and Souza

TABLE 4. Changes in Knee Joint Under Load (50% BW) at 3.0 T MRI

Change* in Parameter	Lateral	Medial	Lateral Contact Region	Medial Contact Region
Tibiofemoral bone gap (%)	1.51 ± 3.0	10.24 ± 6.4	4.01 ± 7.8	6.67 ± 4.3
Femoral cartilage thickness (%)	5.56 ± 6.6	6.28 ± 6.8	5.67 ± 9.4	6.05 ± 8.8
Tibial cartilage thickness (%)	−0.65 ± 5.6	13.07 ± 8.7	−1.49 ± 6.9	9.88 ± 10.2
Femoral cartilage T_2 values (msec)	1.51 ± 1.9	2.08 ± 1.9	2.24 ± 2.3	2.65 ± 2.2
Tibial cartilage T_2 values (msec)	1.38 ± 2.6	2.37 ± 2.3	0.49 ± 2.5	2.29 ± 2.2

*Changes are computed with respect to without knee joint load.

et al[14] are very bulky and may require more setup time. In addition, the proposed device does not comprise any costly MRI-compatible circuitry, such as a load cell reported by Wang et al.[16] Besides, Wang et al[16] used a rod to apply pressure, which might need additional space and may require alteration in the MRI room setting. On the other hand, the device proposed in the current study is easy to use as high ease of donning metric was observed, comprises low-cost components, and does not require any alteration in the MRI room setting; therefore, the proposed device may better suit research studies and regular clinical settings.

One of the advantages of the proposed device is the bidirectional loading mechanism, whereas previously reported[8,14–17] devices can apply the load only from one direction, which may hamper the stability of the experimental setup and cause motion artifact.[17] Wang et al[17] used a camera and marker for such motion correction as an additional resource. However, the proposed device exerted the load from two opposite sides, from the waist and foot sole, so that the net external force on the body is zero; therefore, it brings stability in the experimental setup, which reduces the potential of the motion artifact.

The device was designed at a low cost. Therefore, no high-cost components were used to measure the real-time load during scanning. The load exerted on the knee joint was based on recalibration. Calibration was conducted for 1 kg step load; however, we observed uncertainty in four load cases, where stretched length overlapped with adjacent load (Supplementary material Section 6). Therefore, device resolution was defined for the 2 kg step. The real-time load during scanning could be possible in the future by inclusion of a MRI-compatible devices such as fiber Bragg grating sensors based devices.

The loading device has been successfully tested for MR safety. During the MR safety test, the projectile angular displacement of <45° implies the static magnetic field pull force on the device is less than the gravitation force on the device, and the device is considered MR safe.[32] The proposed loading device can be regarded as MR safe as it exhibits 14° and 36° angular displacement in the static magnetic field of 1.5 T and 3.0 T, respectively. However, in the torque test,[33] the device could be considered MR conditional as torque was not observed in the experiment condition (the device was tied with straps and loaded by subject's leg). The 360° movement of the device (only free device) in the MRI bore was restricted due to the device's size. Therefore, developed torque was not measured but only observed whether it exists inside the MRI scanner. Further, the placement of the device exactly at the is center of the MRI was not possible in the current study setup. However, replacing stainless-steel telescopic channel with titanium or medical graded steel may reduce the developed torque in the device inside the static magnetic field. The device could be considered MR safe because of heat generation due to RF and gradient coil transition exposure, as temperature change was observed <2°C[34] in both the device and phantom. The real-time monitoring of the temperature change was not conducted; it measures with a delay of around 45 seconds. However, real-time temperature monitoring could be done by additional means of MRI-compatible temperature sensors such as fiberoptic or Fluor optic thermometry probes.[34] The standard guidelines are not available to access MR-safety for the proposed device of the current study, as ASTM standards are available for implants. Further, this type of MR safety evaluation is hardly reported in the literature.

Final parameter (TFBG, FCT, TCT, FCT2, TCT2) values evaluated from averaging the large regions on 2D-WearMap[38] may reduce the segmentation error. In the current study, the intra and interobserver variability of ROIs evaluation was smaller than pixel size, which suggests observer consistency. Similarly, the device's ability to reproduce similar loading conditions (measured using FTBG) in the knee during imaging was observed as smaller than pixel size (0.41 mm). Preliminary data of the current study suggest reproducibility of TFGM measurements for the data obtained using with and without loading device. However, this needs to be evaluated on more subjects.

The device's loading behavior was compared to the natural standing stance, using open standing 0.25 T MRI. The device behavior is observed close to stance standing on both legs compared to standing on a single leg stance as "r" > 0.9 for standing both leg stance and "r" < 0.9 for standing single-leg stance; however, correlation is not statistically significant ($P < 0.37$), which might be due to the low number of subjects ($n = 3$).

The loading effect on healthy subjects reported changes in TFBG and FCT due to 50% BW in the range of −5% to 25%,[22] and −1% to 12%,[21,22] respectively, which agrees with the current study. Likewise, the change of T_2-values in healthy cartilage, due to 50%BW, was reported in the range of 0.5–3.5 msec,[14,15,21,24] similar to observed in the current study. The loading effect was observed more prominent in the medial compartment than the lateral compartment in all the parameters. However, the loading effect difference in the compartment in TCT and TCT2 is more than other evaluated parameters may be because of higher thickness than FCT.

Limitations

Firstly, the study had a small number of healthy subjects, particularly for the repeatability study. Another limitation is that durability of the elastic string needs to be checked for long-term use (more than a year). Moreover, the current study calibrated the elastic string up to 45 kg, which limited the weight of the enrolled subject up to 90 kg; as 50% BW is required to apply during the experiment. So, further

calibration of the elastic string is needed for subjects with greater weight. In addition, the exerted load by the device was evaluated during calibration for 15 minutes; other unknown uncertainties that might affect the loading of 50% BW during the MR scanning were not evaluated. In the future, additional components for load measurement during the experiment could be considered for more accuracy. During MRI safety assessment, size of the device restricted the 360° rotation of the device to measure torque. Further, the temperature measurement in this study for MR-safety assessment was not real time. The device was tested only on healthy volunteers. During ROIs selection, there might be some errors (±1 pixel) near the cartilage border; however, we used averaging of cartilage profiles to evaluate parameter values. Averaging should have reduced the effect of these errors. Further studies shall be carried out to include OA patients, particularly early-stage OA.

Conclusions

The device developed in the study could load the knee joint axially with 50% of the body weight during MRI acquisition. The proposed device is portable, easy to insert and remove from the scanner, and can be used in research and regular clinical setting. The novel loading mechanism of the device reduces the potential of motion artifacts and can carry studies related to osteoarthritis, sports, and other knee joint-related researches.

Acknowledgments

The authors would like to thank Dr. Harsh Mahajan for providing the clinical inputs; Mr. Maninder and Ms. Madhuri Bansal for their support in data acquisition; and Dr. Sitikantha Roy for technical inputs. Authors acknowledge the MRI data acquisition support from Mahajan Imaging Centre, New Delhi, India and financial support from Indian Institute of Technology, Delhi, India (FIRP Project No: MI01422).

Conflict of interest

The authors declare that there is no conflict of interest regarding the content of this article.

REFERENCES

1. Eckstein F, Cicuttini F, Raynauld JP, Waterton JC, Peterfy C. Magnetic resonance imaging (MRI) of articular cartilage in knee osteoarthritis (OA): Morphological assessment. Osteoarthr Cartil 2006;14(Suppl 1): 46-75. https://doi.org/10.1016/j.joca.2006.02.026.
2. Boesen M, Ellegaard K, Henriksen M, et al. Osteoarthritis year in review 2016: Imaging. Osteoarthr Cartil 2017;25(2):216-226. https://doi.org/10.1016/j.joca.2016.12.009.
3. De Windt TS, Welsch GH, Brittberg M, et al. Is magnetic resonance imaging reliable in predicting clinical outcome after articular cartilage repair of the knee?: A systematic review and meta-analysis. Am J Sports Med 2013;41(7):1695-1702. https://doi.org/10.1177/0363546512473258.
4. Mackenzie R, Dixon AK, Keene GS, Hollingworth W, Lomas DJ, Villar RN. Magnetic resonance imaging of the knee: Assessment of effectiveness. Brain Lang 1996;51(4):245-250. https://doi.org/10.1016/s0009-9260(96)80340-0.
5. Bruno F, Barile A, Arrigoni F, et al. Weight-bearing MRI of the knee: A review of advantages and limits. Acta Biomed 2018;89:78-88. https://doi.org/10.23750/abm.v89i1-S.7011.
6. Hamada H, Nishii T, Tamura S, Tanaka H, Wakayama T, Sugano N. Comparison of load responsiveness of cartilage T1rho and T2 in porcine knee joints: An experimental loading MRI study. Osteoarthr Cartil 2015;23(10):1776-1779. https://doi.org/10.1016/j.joca.2015.05.019.
7. Musumeci G. The effect of mechanical loading on articular cartilage. J Funct Morphol Kinesiol 2016;1(2):154-161. https://doi.org/10.3390/jfmk1020154.
8. Nag D, Liney GP, Gillespie P, Sherman KP. Quantification of T2 relaxation changes in articular cartilage with in situ mechanical loading of the knee. J Magn Reson Imaging 2004;19(3):317-322. https://doi.org/10.1002/jmri.20000.
9. Bird P, Ejbjerg BO, Lassere M, et al. A multireader reliability study comparing conventional high-field magnetic resonance imaging with extremity low-field MRI in rheumatoid arthritis. J Rheumatol 2007;34(4): 854-856.
10. Blanco RT, Ojala R, Kariniemi J, Perälä J, Niinimäki J, Tervonen O. Interventional and intraoperative MRI at low field scanner - a review. Eur J Radiol 2005;56(2):130-142. https://doi.org/10.1016/j.ejrad.2005.03.033.
11. Ghazinoor S, Crues JV, Crowley C. Low-field musculoskeletal MRI. J Magn Reson Imaging 2007;25(2):234-244. https://doi.org/10.1002/jmri.20854.
12. Kinnunen J, Bondestam S, Kivioja A, et al. Diagnostic performance of low field MRI in acute knee injuries. Magn Reson Imaging 1994;12(8): 1155-1160. https://doi.org/10.1016/0730-725X(94)90080-B.
13. Kladny B, Glückert K, Swoboda B, Beyer W, Weseloh G. Comparison of low-field (0.2 tesla) and high-field (1.5 tesla) magnetic resonance imaging of the knee joint. Arch Orthop Trauma Surg 1995;114(5):281-286. https://doi.org/10.1007/BF00452088.
14. Souza RB, Stehling C, Wyman BT, et al. The effects of acute loading on T1rho and T2 relaxation times of tibiofemoral articular cartilage. Osteoarthr Cartil 2010;18:1557-1563. https://doi.org/10.1016/j.joca.2010.10.001.
15. Nishii T, Kuroda K, Matsuoka Y, Sahara T, Yoshikawa H. Change in knee cartilage T2 in response to mechanical loading. J Magn Reson Imaging 2008;28:175-180. https://doi.org/10.1002/jmri.21418.
16. Wang H, Koff MF, Potter HG, Warren RF, Rodeo SA, Maher SA. An MRI-compatible loading device to assess knee joint cartilage deformation: Effect of preloading and inter-test repeatability. J Biomech 2015; 48(12):2934-2940. https://doi.org/10.1016/j.jbiomech.2015.08.006.
17. Lange T, Maclaren J, Herbst M, et al. Knee cartilage MRI with in situ mechanical loading using prospective motion correction. Magn Reson Med 2014;71(2):516-523. https://doi.org/10.1002/mrm.24679.Knee.
18. Halonen KS, Mononen ME, Jurvelin JS, To J. Deformation of articular cartilage during static loading of a knee joint – Experimental and fi nite element analysis. J Biomech 2014;47:2467-2474. https://doi.org/10.1016/j.jbiomech.2014.04.013.
19. Richard BS, Thomas B, Wu S, et al. Effects of unloading on knee articular cartilage T1rho and T2 magnetic resonance imaging relaxation times: A case series. J Orthop Sport Phys Theray 2012;42(6):511-520. https://doi.org/10.2519/jospt.2012.3975.Effects.
20. Zhang Y, Hunter DJ, Nevitt MC, et al. Association of squatting with increased prevalence of radiographic tibiofemoral knee osteoarthritis the Beijing osteoarthritis study. Arthritis Rheum 2004;50(4):1187-1192. https://doi.org/10.1002/art.20127.
21. Subburaj K, Souza RB, et al. Association of MR relaxation and cartilage deformation in knee osteoarthritis. J Orthop Res 2013;30(6):919-926. https://doi.org/10.1002/jor.22031.Association.

22. Marsh M, Souza RB, Wyman BT, et al. Differences between X-ray and MRI-determined knee cartilage thickness in weight-bearing and non-weight-bearing conditions. Osteoarthr Cartil 2013;21(12):1876-1885. https://doi.org/10.1016/j.joca.2013.09.006.

23. Patel R, Eltgroth M, Souza R, et al. Loaded versus unloaded magnetic resonance imaging (MRI) of the knee: Effect on meniscus extrusion in healthy volunteers and patients with osteoarthritis. Eur J Radiol Open 2016;3:100-107. https://doi.org/10.1016/j.ejro.2016.05.002.

24. Souza RB, Kumar D, Calixto N, et al. Response of knee cartilage T 1rho and T 2 relaxation times to invivo mechanical loading in individuals with and without knee osteoarthritis. Osteoarthr Cartil 2014;22(10): 1367-1376. https://doi.org/10.1016/j.joca.2014.04.017.

25. Stehling C, Souza RB, Le Graverand M-PH, Wyman BT, Li X, Majumdar S. Loading of the knee during 3.0 T MRI is associated with significantly increased medial meniscus extrusion in mild and moderate osteoarthritis. Eur J Radiol 2012;81(8):1839-1845.

26. Van Rossom S, Smith CR, Zevenbergen L, et al. Knee cartilage thickness, T1ρ and T2 relaxation time are related to articular cartilage loading in healthy adults. PLOS ONE. 2017;12:1:e0170002. https://doi.org/10.1371/journal.pone.0170002.

27. Stehling C, Souza RB, Le Graverand MP, et al. Loading of the knee during 3.0 T MRI is associated with significantly increased medial meniscus extrusion in mild and moderate osteoarthritis. Eur J Radiol 2012 Aug 1; 81(8):1839-1845.

28. Shapiro LM, Gold GE. MRI of weight bearing and movement. Osteoarthr Cartil 2012;20(2):69-78.

29. Draper CE, Besier TF, Fredericson M, et al. Differences in patellofemoral kinematics between weight-bearing and non-weight-bearing conditions in patients with patellofemoral pain. J Orthop Res 2011 Mar;29(3):312-317.

30. McWalter EJ, Hunter DJ, Wilson DR. The effect of load magnitude on three-dimensional patellar kinematics in vivo. J Biomech 2010;43(10): 1890-1897.

31. Powers CM, Ward SR, Fredericson M, Guillet M, Shellock FG. Patellofemoral kinematics during weight-bearing and non-weight-bearing knee extension in persons with lateral subluxation of the patella: A preliminary study. J Orthopaed Sports Phys Therapy 2003; 33(11):677-685.

32. ASTM. *F2052-15, standard test method for measurement of magnetically induced displacement force on medical devices in the magnetic resonance environment*. West Conshohocken, PA: ASTM International; 2015.

33. ASTM. *F2213-17, standard test method for measurement of magnetically induced torque on medical devices in the magnetic resonance environment*. West Conshohocken, PA: ASTM International; 2017. www.astm.org.

34. ASTM. *F2182-19e2, standard test method for measurement of radio frequency induced heating on or near passive implants during magnetic resonance imaging*. West Conshohocken, PA: ASTM International; 2019. www.astm.org.

35. Burnham KP, Anderson DR. Multimodel inference: Understanding AIC and BIC in model selection. Sociol Methods Res 2004;33(2):261-304.

36. Wang Z, Bovik AC, Sheikh HR, Simoncelli EP. Image quality assessment: From error visibility to structural similarity. IEEE Trans Image Process 2004;13(4):600-612.

37. Thaha R, Jogi SP, Rajan S, Mahajan V, Mehndiratta A, Singh A. A semi-automatic framework based upon quantitative analysis of MR-images for classification of femur cartilage into asymptomatic, early OA, and advanced-OA groups. Journal of Orthopaedic Research. 2021. https://doi.org/10.1002/jor.25109.

38. Popović ZB, Thomas JD. Assessing observer variability: A user's guide. Cardiovasc Diagn Therapy 2017;7(3):317.

39. Jogi SP, Thaha R, Rajan S, et al. Model for in-vivo estimation of stiffness of tibiofemoral joint using MR imaging and FEM analysis. J Transl Med 2021;19:310. https://doi.org/10.1186/s12967-021-02977-1.

40. Chan DD, Cai L, Butz KD, Trippel SB, Nauman EA, Neu CP. In vivo articular cartilage deformation: Noninvasive quantification of intratissue strain during joint contact in the human knee. Sci Rep 2016;6(1):1-14.